Calcium and Hydrogen on Graphene as a Mechanism for Hydrogen Storage

Erik Swenson

A senior thesis submitted to the faculty of
Brigham Young University
in partial fulfillment of the requirements for the degree of

Bachelor of Science

Bret Hess, Advisor

Department of Physics and Astronomy

Brigham Young University

April 2016

ABSTRACT

Calcium and Hydrogen on Graphene as a Mechanism for Hydrogen Storage

Erik Swenson
Department of Physics and Astronomy, BYU
Bachelor of Science

Because of its status as an emerging energy carrier, methods of hydrogen storage are in high demand. Using computational methods, we explore a very large space of graphene structures with different adsorption configurations of hydrogen and calcium as mechanisms for hydrogen storage. We expand our search space further than the traditional search space by using cluster expansion to enumerate structures in a variety of computational cell shapes and sizes. This allows for periodicity not studied previously. We compare the results found using this type of enumeration with results obtained in other work and we present the most energetically favorable structures found in our search.

Contents

List of Figures

Chapter 1

Introduction

1.1 Motivation

In the search for a source of abundant, renewable, clean energy, molecular hydrogen as a fuel source has emerged as a promising alternative to hydrocarbons. Standard hydrocarbon fuel sources such as gasoline or propane give off CO_2 as a byproduct. Both production and consumption of hydrocarbon fuels can pose a risk to the people or the environment in densely populated cities or highly industrialized areas where these activities are prominent. It is for this reason that hydrocarbon fuel is becoming less and less desirable in a world where the need for energy rapidly continues to grow.

We are not claiming that a molecular hydrogen fuel source will completely solve this problem. After all, to *produce* the fuel, we somehow need to obtain and isolate the hydrogen molecules which requires some other energy source (*e.g.* electricity). The *consumption*, however, is much cleaner. When hydrocarbons are burned, CO_2 is formed as the carbon bonds break and oxygenate. On the other hand, consumption of molecular hydrogen results in completely benign H_2O when the hydrogen bonds break and oxygenate, posing much less of a threat to the surrounding areas.

The great advantage, then, of hydrogen fuels comes when the production plants can be relocated to remote areas outside the cities while only consumption occurs inside the cities. This somewhat isolates the inhabitants of the cities from the harmful pollutants associated with fuel production.

Finding an efficient and practical way to store hydrogen in large enough amounts for use as fuel now becomes the intriguing problem. From a molecular perspective, we need a structure that is stable and binds molecular hydrogen, yet simple enough to manufacture in bulk amounts.

1.2 Graphene and Hydrogen Storage

Graphene, an essentially two-dimensional hexagonal lattice of carbon atoms, was discovered in 2004 .[1] Graphene itself is incredibly strong, very thin, and an extremely good conductor of heat and electricty .[2] The high density of potentially bond-forming atoms and the two-dimensional nature of the material make graphene a natural starting point for hydrogen storage applications .[3] In fact, graphene has already proven to bond with atomic hydrogen in the form of a derivative structure called *graphane* .[4,5] This structure forms when a hydrogen atom bonds, or adsorbs, to each of the carbon atoms in the lattice. Throughout this paper, we will refer to any of these adsorption atoms bonded directly to the carbon monolayer as "adatoms". In the graphane structure, the hydrogen atoms bond with both sides of the graphene sheet in an alternating top-bottom fashion (see Figure 1.1). A slight "buckling" is introduced to the lattice as a result of this bonding.

However, graphane by itself is not very useful for hydrogen storage even though it provides a hydrogen atom for every carbon atom in the lattice. Graphane is a very stable structure which makes extracting the hydrogen atoms an energy consuming task. To break the strong, covalent bonds ($\sim$6.56 eV / atom [4]) that have formed between the carbon and hydrogen atoms, we would have to heat the structure—again drawing from another energy source—to the point that the energy lost balances the energy gained. Even if there was some way to easily extract the hydrogen atoms,

(a) Side View

(b) Top View
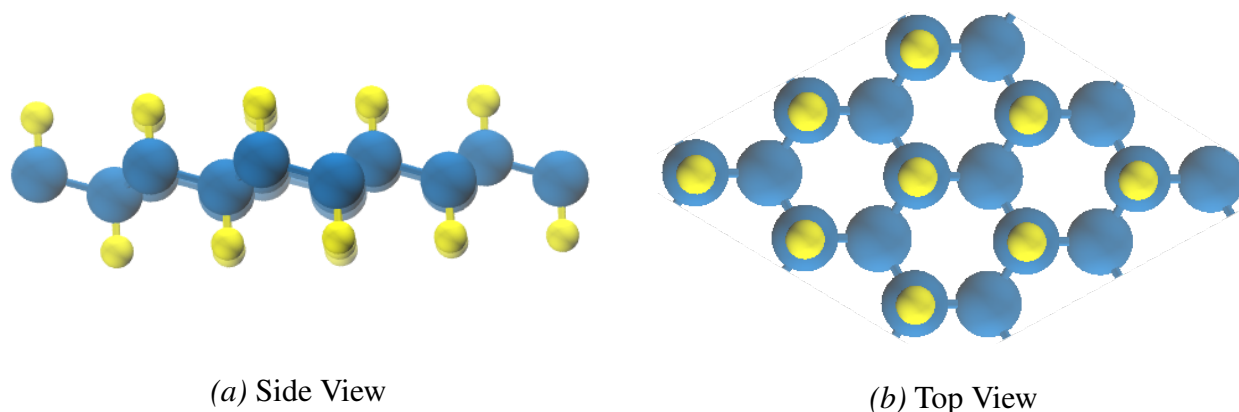
Figure 1.1 Diagram of Graphane Structure

A visual depiction of the graphane structure. Note the alternating above-below scheme and lattice buckling apparent in *(a)*.

they would tend to form bonds with each other as soon as they were far enough away from the carbon monolayer, releasing the energy we want to harvest during the formation of the H_2 bond. All that aside, atomic hydrogen (H) is much less useful as a fuel source than molecular hydrogen (H_2). We need a structure that binds pre- formed hydrogen molecules and, because of its stability, graphane does not.

We can remedy this problem by making a small modification to the graphane structure. If we replace some of the hydrogen adatoms with metal atoms, we can create a structure that might bind a reasonable amount of molecular hydrogen.

Computational work has already performed examining calcium and lithium as the adatoms with promising results. Hussain *et al.* have explored both of these metals and report a hydrogen storage capacity of 6 wt. % for calcium[6] and 12 wt. % for lithium,[7–10] both with reasonable adsorption energies.

1.3   Our Project

In this paper, we also explore computationally the possibility of using a graphene monolayer doped with calcium and hydrogen as a practical solution to the hydrogen storage problem. However, our work goes beyond the work that has previously been carried out in two ways.

Firstly, we allow for "vacancies"—carbon sites with no corresponding atom in the adsorbant monolayer. With vacancies in the structure, the adatoms may have the ability to interact with more of the carbon atoms, producing higher binding energies between the carbon layer and the adatom layer. More space between the adatoms might also reduce the tendency to cluster, a persistent plague in the hydrogen storage field.

Secondly, we examine structures from a multitude of computational (unit) cell sizes and shapes. This adds a significant degree of complexity to structure enumeration, but other members of our group have developed methods to speed up the computation. Traditionally, only one diamond-shaped unit cell has been studied which greatly limits the possible atomic configurations that can be acheived. We use the UNiversal CLuster Expansion (UNCLE)[11] code to enumerate many different cell shapes that contain the same number of atoms as the traditional unit cell (see Figure 1.2). By using this type of structure enumeration, we hope to discover new structures with promising energetics.

We begin by briefly summarizing some key concepts and providing definitions for important terms. We will outline the computational algorithms used for structure enumeration, selection, and prioritization. We conclude with a presentation of the results we obtained. We compare structures with no vacancies against structures with vacancies and analyze what we find by searching a variety of cell shapes and sizes. We also make mention of several directions for future work in the field, many of which are currently being explored by our group.

(a) Volume 4 (2×2)

(b) Volume 5 (1×5)

(c) Volume 7 (1×7)

(d) Volume 9 (3×3)
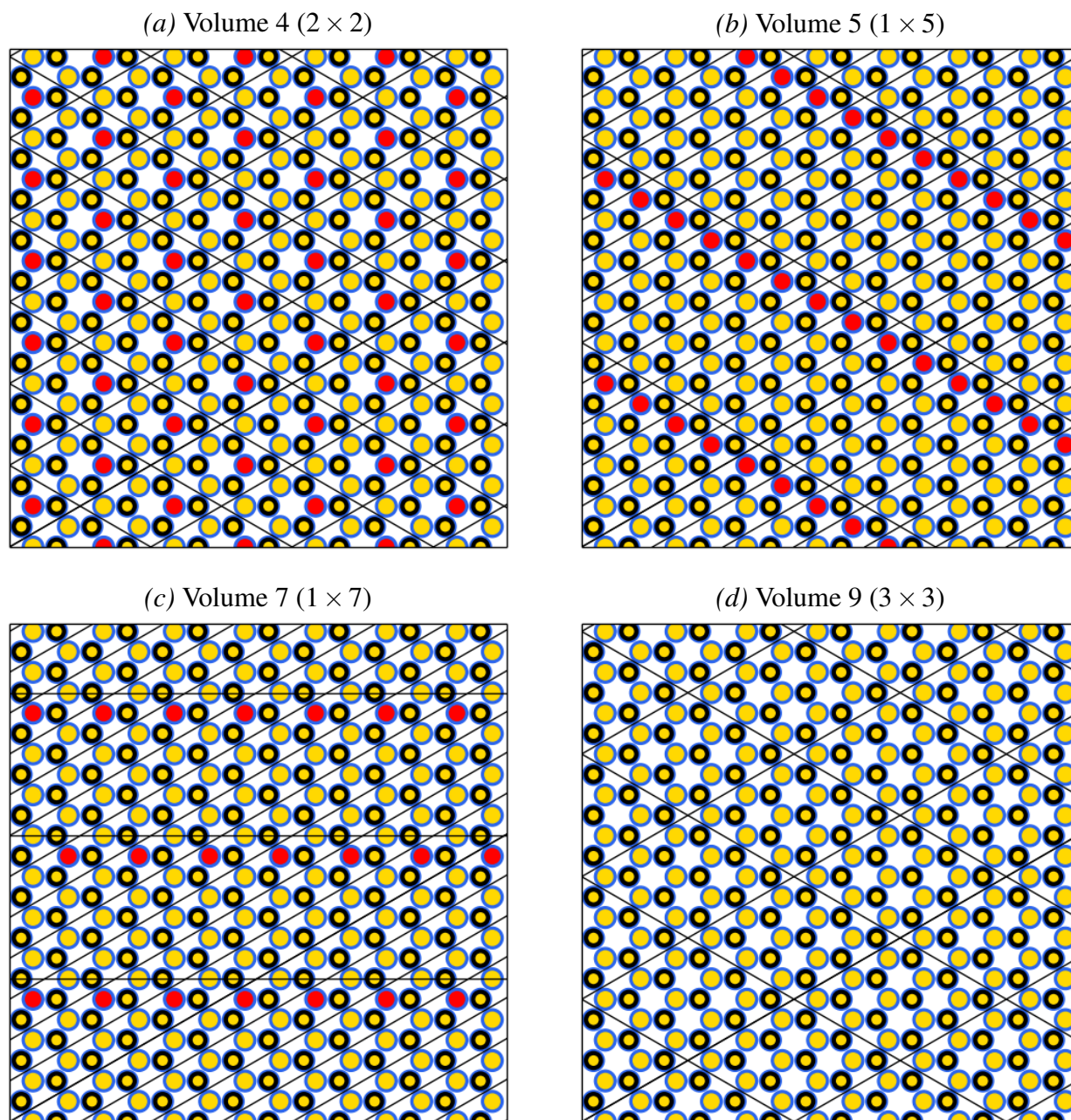
Figure 1.2 Examples of the different computational unit cells used in structure enumeration. The cells are defined by the periodic black lines in the drawings. The blue circles represent carbon atoms in the graphene lattice. Yellow and red circles represent hydrogen and calcium adatoms respectively. A thick border around an adatom signifies that the atom is below the plane. Note that the structure in *(d)* is a two-dimensional representation of the same structure pictured in Figure 1.1.

Chapter 2

Methods

2.1 Methods Common to Other Groups

2.1.1 Density Functional Theory

We ran simulations using the Vienna Ab-Initio Simulations Package (VASP)[12–15] code which peforms calculations based on Density Functional Theory (DFT). DFT, as the name suggests, uses functionals of electron density to model atoms and their interactions (citation). In the simplest of terms, a *functional* is a function of another function. In other words, it is a function that takes in a vector and maps it to a scalar. In the case of modeling molecular structure energetics, the energy functional is of greatest interest. It takes in the electron density function at a given point and returns a scalar energy value. To find energetically favorable structures, then, the goal is to minimize the energy functional for each structure.

A drawback to DFT is that it is somewhat inaccurate in the calculation of weak van Der Waals forces which play a large role in the carbon-hydrogen-metal systems being studied (citation). At the heart of this problem is the fact that VASP makes use of two notable approximations to increase computational speed. In the Local Density Approximation (LDA), the energy functional

only depends on the density at the point where the functional is being evaluated. A slightly modified approach called the Generalized Gradient Approximation (GGA) is similar except that it also takes into account the gradient of the density at the point being evaluated. Both of these approximations have been shown to inaccurately represent the van Der Waals interactions, with LDA overestimating and GGA underestimating.[6] That being said, for simulations with more than just a few atoms, these methods are industry standards and the best that we can do.

2.1.2 Cluster Expansion

Cluster Expansion (CE) provides a mathematical model from which we can predict the energies of a comprehensive space of structures based on the calculated energies of a few structures. CE gets its name from the "clusters", or combinations of occupied sites, that are summed together to represent a structure. Each cluster has an associated weight term which represents energy in this case. Clusters and their weights model the interaction between the atoms that make up the cluster. Clusters can be defined by a single atom (a 1-body cluster) or include any number of atoms in the lattice (an n-body cluster). As we include more clusters, the accuracy of the model increases until, in the limit of including all possible structures, it approaches the actual energy of the structure. However, we can obtain excellent results even with a significant truncation. UNCLE truncates the expansion after 6-body clusters.

The cluster expansion model is defined by the following equation:

$$E_\sigma = \sum_c \Pi_{\sigma c} J_c \tag{2.1}$$

where σ represents a particular structure and c represents a particular cluster. The E_σ term represents the known (calculated) energy of the structure σ. The Π matrix is a matrix of correlation values between structures and clusters. The rows in the matrix represent structures and the columns represent clusters. Finally, the J_c term is an energy "weight" for a given cluster. For visualization's

sake, it may be easier to understand in matrix form.

$$
\begin{bmatrix} E_1 \\ E_2 \\ \vdots \\ E_n \end{bmatrix} = \begin{bmatrix} \Pi_{11} & \Pi_{12} & \cdots & \Pi_{1m} \\ \Pi_{21} & \Pi_{22} & \cdots & \Pi_{2m} \\ \vdots & \vdots & \ddots & \vdots \\ \Pi_{n1} & \Pi_{n2} & \cdots & \Pi_{nm} \end{bmatrix} \begin{bmatrix} J_1 \\ J_2 \\ \vdots \\ J_m \end{bmatrix}
\tag{2.2}
$$

In other words, the energy of a given structure is simply the sum of the properly weighted terms in the row of the Π matrix that represents the structure. If the Π matrix were square, we could simply invert the matrix and multiply to find the weights. However, the number of clusters and the number of structures do not have to be (and rarely are) equivalent. This generally results in a an underdetermined system for our purposes and more complex linear algebra techniques are required to solve it. Fortunately, Nelson *et al.* have developed Bayesian Compressed Sensing methods to solve this system efficiently.[16]

Once the weights are found, the multiplication on the right side of Eq. 2.1 predicts the energy for any structure in the space.

2.2 Enumeration of Structures

We use the UNCLE code to perform enumeration of all possible symmetrically inequivalent structures in a given space. UNCLE performs a solely mathematical enumeration based on the shape of the lattice and the adatom options at each lattice site. This type of enumeration will inevitably produce structures that could not possibly exist in nature due to the size of the adatoms. For example, because the atomic radius of a calcium atom is large ($\sim$1.74 Å) and carbon-carbon bond lengths in the graphene lattice are not ($\sim$1.42 Å), we cannot place two calcium atoms adjacent to one another. Pairs of atoms that cannot be placed next to each other are termed *forbidden pairs*. We do not want to waste time in the search running "forbidden" structures through VASP calculations so, to this

end, other members of our group have added functionality to exclude them from the enumeration (reference Joseph's paper).

Our enumeration, however, is left somewhat incomplete. From sets of structures that are rotationally or translationally equivalent (like 10 and 01) we only keep one. We then use *tiles* of the remaining symmetrically inequivalent structures to build up our computational unit cells. Because we form the tiles after elimination by symmetry, some tiles are not available for use and, thus, some structures are left out of the enumeration. This does have a positive consequence, though, in that we can perform higher volume enumerations and explore higher volume structures in our search than we could otherwise.

2.3   Search for Favorable Structures

The main portion of my work in the group dealt with creating, coding, and automating the iterative process of searching the space of possible structures. The basic algorithm can be seen in Figure 2.1. It starts by selecting a set of what are called independently and identically distributed (IID) structures to use as initial input to the iteration loop. IID means that the initial set will include structures that are as different as possible from one another.

Our new code takes the IID structure set and extracts the important information into a format that VASP can work with. VASP iteratively makes slight adjustments to the positions of the ions and the electrons in order to minimize the energy of the structure in a process called *relaxation*.

Once VASP has found the energy-minimized configuration for each structure, we create a CE model based on the results from this initial structure set. The model predicts the energy of all the structures in the space. (Initially, this model is not very accurate, but as we add more structures to the model each iteration, the accuracy increases substantially.) We prioritize the structures according to a decaying exponential scale. Energetically favorable (low energy) structures are
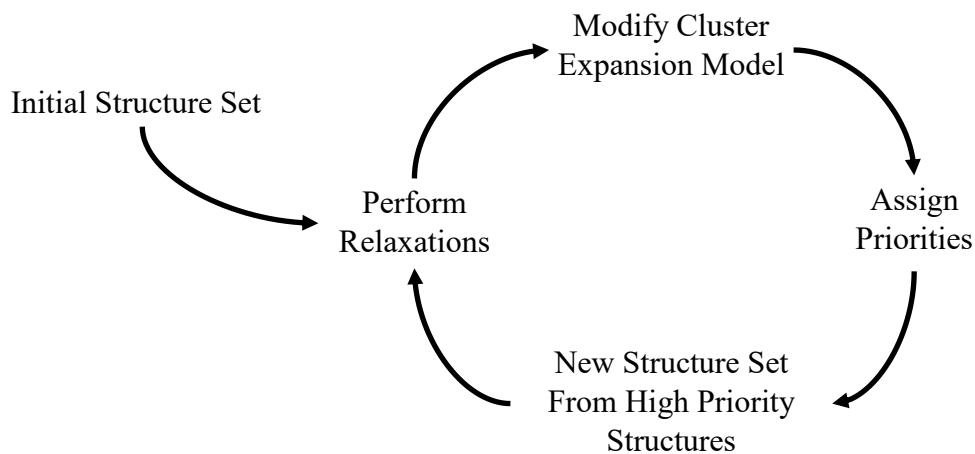
Figure 2.1 A high level map of the iteration process. We start with a randomly selected set of structures. We run the structures through atomic and electronic relaxation routines and use that data to create a predictive model for all possible structures. We then assign each structure a priority and choose a set of highest priority to run back through the loop.

given high priority while high energy structures are given a much lower priority.

We then select a new set of the highest priority structures from the pool of structures that have not been run through VASP calculations and the loop begins again. It should be noted that, because we choose new structures at the end of each iteration based on their priority, the energy-predictive model we refine may not be very accurate for higher energy structures. This is not an issue since high energy structures are of no practical interest to us anyway.

Chapter 3

Results

3.1 Energy Metrics

When analyzing the results of our energy calculations, the most intuitive metric we use to summarize a structure's energy is what we have termed formation energy. Formation energy (FE) is defined as the average energy per atom required to pull an adatom out of a reference structure containing only that particular atom and bind it to the graphene layer. For hydrogen, we use a hydrogen molecule (H_2) as the reference structure and for calcium, the reference structure is a hexagonal monolayer of Ca atoms bound together. Mathematically,

$$FE_{struct} = E_{struct} - \left(E_{graphene} + \sum_i N_i E_i^{ref} \right) \tag{3.1}$$

where E_{struct} is the energy value of that structure directly from the calculations, $E_{graphene}$ is the calculated reference energy of the graphene, and the summation term gives the number of each type of adatom multiplied by its corresponding reference energy.

Another important metric used in our analysis is planar binding energy (PBE) which, in the most simple terms, tells us how much energy is required to separate the adatom layer from the carbon monolayer far enough that the interaction between the two layers is negligible. Structures

with positive or weakly negative PBE are essentially already separated into layers. Mathematically,

$$PBE_{struct} = E_{struct} - \left(E_{graphene} + E_{adatoms} \right) \tag{3.2}$$

where E_{struct} and $E_{graphene}$ carry the same meaning as in FE and $E_{adatoms}$ represents the total energy of the isolated adatom layer.

Our goal is to find structures that exhibit a strong FE as well as a strong PBE. To this end, we have defined a third, non-physical quantity called sorting energy (SE) which is defined as

$$SE_{struct} = max \left(FE_{struct}, PBE_{struct} \right) \quad . \tag{3.3}$$

When we sort the structures according to their SE, we can easily find those that have strong FE as well as PBE.

Figure 3.1 shows a plot of PBE vs. FE for volume nine structures where vacancies are allowed. We can see that the region of interest representing structures that simultaneously boast low FE and PBE is very sparsely populated. In fact, the small trail of structures on the far left hand side that dip down into this region are all "graphane-like" in that they only contain hydrogen atoms bonded to the carbon monolayer. Since these structures have no calcium content and, hence, no way to bind hydrogen molecules, they are of no practical interest to us for hydrogen storage applications. Our focus will be on the other structures that border this empty region even though their overall energetics may be higher than we had hoped for.

3.2   Single-Sided Bonding

In the single-sided case, we find many structures with strong FE as well as PBE. The structures with the lowest SE, however, contain high calcium concentrations and show signs of clustering perpendicular to the carbon monolayer rather than binding directly to the monolayer. This is not too surprising for single-sided bonding since we would expect calcium atoms that are in close proximity to each other to form bonds of their own rather than with the carbon atoms.
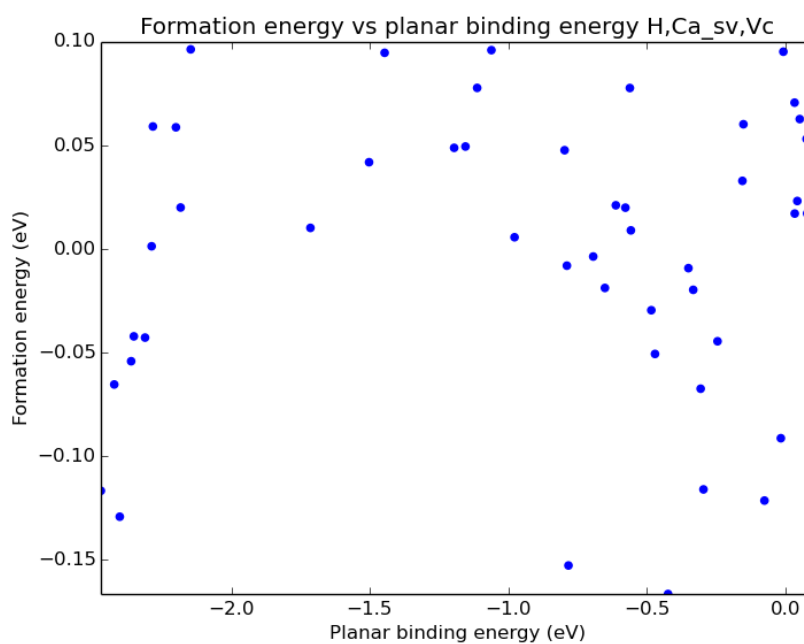
Figure 3.1 A plot of formation energy vs. planar binding energy for volume 9 double-sided structures. Each blue dot represents a particular structure. Ignoring the tail of "graphane-like" structures at the far left side of the plot, note the large gap in the region of strong FE and PBE where very desirable structures would appear.
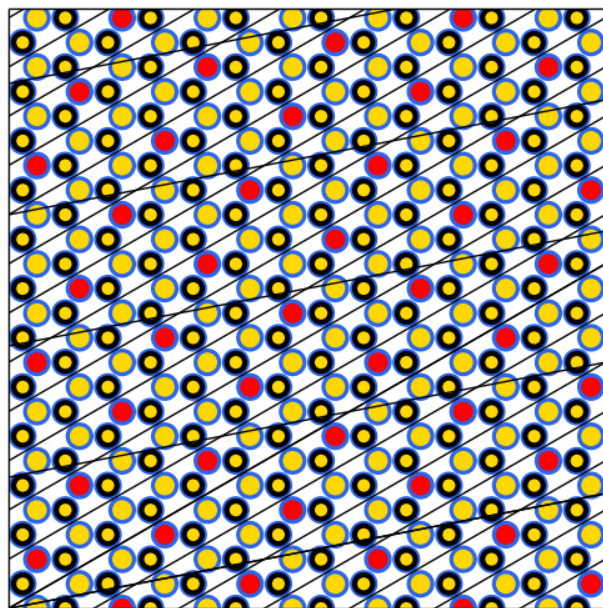
Figure 3.2 Structure S1, the lowest energy structure in the single-sided search that contains calcium atoms and does not suffer from calcium clustering.

Calcium clustering causes two main problems. Firstly, the clustered calcium atoms create strong bonds with each other, reducing the ability to bind H_2 to the structure. Secondly, even if the calcium clusters could still bind H_2, the cluster takes up more space, resulting in a much less space-efficient structure for hydrogen storage.

The lowest energy single-sided structure found in our search that did not suffer from calcium clustering is shown in Figure 3.2. We will call this structure S1. The calcium atoms in S1 are spaced far enough apart so as to avoid interacting too strongly with each other. Table 3.1 shows the four lowest energy structures in the single-sided search excluding graphane-like structures and structures that suffer from calcium clustering. Notice that these structures all have FE in the range of ~ -0.8 eV and PBE in the range of ~ -2.3 eV with the exception of structure S4 having PBE $= -2.899$ eV.

Structure	Volume	SE (eV / atom)	FE (eV / atom)	PBE (eV / atom)
S1	8	-0.815	-0.815	-2.271
S2	8	-0.806	-0.806	-2.322
S3	8	-0.804	-0.804	-2.316
S4	8	-0.804	-0.804	-2.899

Table 3.1 The four structures with the lowest sorting energy for a single-sided H-Ca system.

3.3   Double-Sided Bonding

[*Insert results from binary double-sided bonding and compare with the structure from the paper.*]

3.4   Effect of Vacancies

[*Insert results from ternary single-sided and compare with binary single-sided.*]

[*Insert results from ternary double-sided and compare with binary double-sided.*]

[*This is made up, but it would be really cool.*] The comparisons made above, show that vacancies play an important role in the formation of structures for hydrogen storage. We have shown that vacancies allow for higher concentrations of calcium atoms without giving way to clustering. This is a desirable characteristic because, theoretically, structures with a higher concentration of calcium should be able to bind more hydrogen and, therefore, be better suited to hydrogen storage applications.

3.5   Variation of Unit Cells

It is clear that the size and shape of the computational unit cell used is an important parameter in the search for low energy structures. In the single-sided search not allowing vacancies—the search where having a large cell size should matter the most—the highest ranking of any structure of the 3×3 unit cell type pictured in Figure 1.2 *(d)* was 29th. Out of the 100 lowest energy structures in the search, only *30* were volume nine structures and, of those thirty, only *eight* had 3×3 unit cells. Interestingly enough, 49 of the lowest 100 came from volume eight unit cells. Most of the low energy structures had a longer, stretched unit cell like the one pictured in Figure 1.2 *(c)*. This is probably because spreading the calcium atoms out farther from each other decreases their interaction with each other and increases their interaction with the graphene monolayer.

This result strongly suggests that the periodicities encompassed by the volume nine, 3×3 unit cell are not ideal periodicities for a H-Ca system. In any case, it is an important illustration of the fact that, in order to perform a complete search of the space, the size and shape of the unit cell must be a parameter in the search.

Appendix A

Appendix Title

You can put supplimentary content in an appendix.

Bibliography

[1] K. S. Novoselov, A. K. Geim, S. V. Morozov, D. Jiang, Y. Zhang, S. V. Dubonos, I. V. Crigorieva, and A. A. Firsov, "Electric Field Effect in Atomically Thin Carbon Films.," Science **306,** 666 – 669 (2004).

[2] C. Lee, X. Wei, J. W. Kysar, and J. Hone, "Measurement of the Elastic Properties and Intrinsic Strength of Monolayer Graphene," Science **321,** 385–388 (2008).

[3] M. Pumera, "Graphene-based nanomaterials for energy storage," Energy & Environmental Science **4,** 668–674 (2011).

[4] J. O. Sofo, A. S. Chaudhari, and G. D. Barber, "Graphane: A two-dimensional hydrocarbon," Physical Review B 75 (2007).

[5] D. C. Elias *et al.*, "Control of Graphene's Properties by Reversible Hydrogenation: Evidence for Graphane," Science **323,** 610–613 (2009).

[6] T. Hussain, B. Pathak, M. Ramzan, T. A. Maark, and R. Ahuja, "Calcium doped graphane as a hydrogen storage material," Applied Physics Letters 100 (2012).

[7] T. Hussain, A. De Sarkar, and R. Ahuja, "Strain induced lithium functionalized graphane as a high capacity hydrogen storage material," APPLIED PHYSICS LETTERS 101 (2012).

[8] T. Hussain, T. Adit Maark, A. De Sarkar, and R. Ahuja, "Polylithiated (OLi2) functionalized graphane as a potential hydrogen storage material," Applied Physics Letters 101 (2012).

[9] T. Hussain, A. D. Sarkar, and R. Ahuja, "Functionalization of hydrogenated graphene by polylithiated species for efficient hydrogen storage," International Journal of Hydrogen Energy **39,** 2560 – 2566 (2014).

[10] T. Hussain, B. Pathak, T. A. Maark, C. M. Araujo, R. H. Scheicher, and R. Ahuja, "Ab initio study of lithium-doped graphane for hydrogen storage," EPL 96 (2011).

[11] D. Lerch, O. Wieckhorst, G. L. W. Hart, R. W. Forcade, and S. MÃijller, "UNCLE: a code for constructing cluster expansions for arbitrary lattices with minimal user-input," Modelling and Simulation in Materials Science and Engineering **17,** 055003 (2009).

[12] G. Kresse, "Ab initio molecular dynamics for liquid metals," Journal of Non-Crystalline Solids **192âĂŞ193,** 222 – 229 (1995), structure of Non-Crystalline Materials 6.

[13] G. Kresse and J. Hafner, "*Ab initio* molecular-dynamics simulation of the liquid-metal–amorphous-semiconductor transition in germanium," Phys. Rev. B **49,** 14251–14269 (1994).

[14] G. Kresse and J. FurthmÃijller, "Efficiency of ab-initio total energy calculations for metals and semiconductors using a plane-wave basis set," Computational Materials Science **6,** 15 – 50 (1996).

[15] G. Kresse and J. FurthmÃijller, "Efficient iterative schemes for *ab initio* total-energy calculations using a plane-wave basis set," Phys. Rev. B **54,** 11169–11186 (1996).

[16] L. J. Nelson, V. Ozoliņš, C. S. Reese, F. Zhou, and G. L. W. Hart, "Cluster expansion made easy with Bayesian compressive sensing," Phys. Rev. B **88,** 155105 (2013).